Mesua Ferrea L. Seed Oil Modified Sulfone Epoxy Resin and Multi-Walled Carbon Nanotube Nanocomposites and Their Biomedical and Mechanical Properties

Article *in* Journal of Computational and Theoretical Nanoscience · March 2012

DOI: 10.1166/asl.2012.2022

CITATIONS
2

READS
180

3 authors, including:

Gautam Das
Gachon University
51 PUBLICATIONS **1,132** CITATIONS

SEE PROFILE

Niranjan Karak
Tezpur University
282 PUBLICATIONS **8,755** CITATIONS

SEE PROFILE

RESEARCH ARTICLE

Advanced Science Letters
Vol. 4, 1–9, 2012

Mesua Ferrea L. Seed Oil Modified Sulfone Epoxy Resin and Multi-Walled Carbon Nanotube Nanocomposites and Their Biomedical and Mechanical Properties

Gautam Das[1], Jetendra K. Roy[2], Ashis K. Mukherjee[2], and Niranjan Karak[1,*]

[1]*Advanced Polymer and Nanomaterial Laboratory, Chemical Sciences Department, Tezpur University, Napaam-784028, India*
[2]*Department of Molecular Biology and Biotechnology, Tezpur University, Napaam-784028, India*

Adhesive strength of multiwalled carbon nanotubes/*Mesua ferrea* L. seed oil based sulfonated epoxy resin nanocomposites was investigated by lap shear method on different substrates (wood/aluminium/polypropylene). MWCNT was functionalized by mild oxidative technique using phase transfer catalyst (PTC). The modification was confirmed by FTIR technique, whereas the stability of the dispersion of MWCNT in polar aprotic solvents confirms the functionalization. *Bacillus subtilis* bacterial strain was used for the first time to study the biodegradation of the epoxy/MWCNT nanocomposites. The increase in the statistical growth of bacteria on the nanocomposites determined by the bacterial OD (optical density) measurement confirms bacterial colonization at the expense of degradation of the systems. The biodegradability of the nanocomposites was observed to increase with the increase of MWCNT loading. Further RBC haemolytic protection assay test of the nanocomposites confirm their cyto-compatibility. Nanocomposite with 3 wt% loading exhibit about 161 percent enhancement in adhesive strength for wood substrate and about 156.6 percent enhancement in tensile strength. The thermal stability of the nanocomposites enhances with MWCNT loadings and 3 wt% MWCNT loading exhibited 41 °C improvements over the pristine polymer. The results indicate the potentiality of MWCNT/epoxy nanocomposite as advanced biomedical adhesive.

Keywords: Carbon Nanotubes, Adhesive Strength, Biodegradation, Renewable Resources, Epoxy Resin.

1. INTRODUCTION

The proper selection of an adhesive for biomedical application in contemporary technology is multidisciplinary and challenging to extreme.[1,2] The type and state of an adhesive, its working properties, the temperature and time required for its curing influences the choice of process for producing good bonded structure. Epoxy resin based on bisphenol-A plays an important role in several technologies such as adhesive tapes, machine part assembly, composite materials, tyres etc. because of its excellent thermal, mechanical and adhesive characteristics.[3–5] However due to its extensive brittleness and non cyto-compatibility the monolithic applications in biomedical field is restricted.[6] Joint durability is another factor that has been one of the major concerns for application under humid condition (*in vitro*) as it usually suffers from non uniform distribution of stress over the continuous bonded area and subsequently deterioration of properties.[7] Therefore, it is necessary to develop high performance epoxy adhesives that can overcome the current problems to meet the requirements of different applications including biomedical

The adhesive compositions to be useful for biomedical application must be non-toxic, adhere to moist tissue at body temperature and economically satisfactory.[4] Thus, the development of biocompatible bonding agents with good structural properties is a relevant aspect of the success of these materials in biomedical field.[8–11]

Bio-based polymers have gained lots of interest in recent times; this evolution has revolutionized the retro thinking about the products obtained from renewable resources. Indeed the current opportunities of bio-based polymer nanocomposites in biomedical applications may arise from the potentiality for vast multitude of applications and different functional requirements.[12,13] In this pursuit bio-based epoxy resin has been viewed as a potential substitute to the more conventional epoxy

*Author to whom correspondence should be addressed.

system. However, vegetable oil based epoxy generally is often attributed with weak mechanical properties[14, 15] and is a challenge to the material scientists.

In this regard, the use of carbon nanotubes (CNT) as nanofillers might be one of the best options due to their intrinsic extraordinary thermal and mechanical properties.[16–18] MWCNT diameters ranging from 20–30 nm and an aerial density 10^{10}–10^{11} tubes/cm^2, an estimate based on the Johnson–Kendall–Roberts theory[19] suggests that it is possible to generate adhesive strengths of more than 500 N/cm^2. However, for efficient reinforcement of CNT, two main issues are widely recognized as being critical: (i) homogeneous dispersion of the nanofiller within the polymer matrix, and (ii) strong interfacial bonding between the nanofiller and the matrix. Several research works have recently been devoted to reinforcement of epoxy matrices with functionalized carbon nanotubes.[20–22] In spite of the aggressive work that has been lately dedicated to this topic, it is recognized that the experimental results are still not convergent and more researches are needed in order to shed light on the development of the nanocomposites with acceptable properties[23] in this field.

Mesua ferrea L. (70% oil content) seed oil is abundantly found in the north-eastern part of the country, several literature reports on exploitation of this oil in production of eco-friendly polymers.[24–25] This oil was used as the raw material for the synthesis of sulfone based epoxy resin. Vegetable oil based sulfone epoxy has many added advantages as described in earlier report.[14] The polar functionalities of *Mesua ferrea* L. seed oil based epoxy may increase the physiochemical interaction with the functionalized MWCNT. Subsequently this may aid to good interfacial bonding between the nanofiller and the matrix.

In this paper the author reports the modification of MWCNT using mild oxidative technique and preparation of nanocomposites using *Mesua ferrea* L. seed oil based sulfone epoxy as the matrix. The mechanical properties, adhesive strength and also thermal stability of the nanocomposites were studied at different MWCNT loadings. The biodegradability test on epoxy and the nanocomposites were carried out using *Bacillus subtilis* for the first time; further RBC haemolysis assay was studied in order to examine the feasibility of these nanocomposites as biomedical adhesive.

2. EXPERIMENTAL DETAILS

2.1. Materials

Mesua ferrea L. (Nahar) seeds (Jamugurihat, Assam) were utilized for extraction of the oil. MWCNTs with diameter and length of about 10–20 nm and 20 μm, respectively, were purchased from Iiljin Nanotech., Korea. Epichlorohydrin, Acetic acid, Cetrimide (Merck, Mumbai, India), Potassium dichromate (Ranbaxy, New Delhi, India) and Bis(4-hydroxy phenyl) sulfone (Aldrich, Germany) were used as received. Bisphenol-A (BG and Co., India) was used after purification by recrystalization from toluene. All other reagents used in the present investigation were reagent grade.

2.2. Purification and Modification of Pristine MWCNT

The modified protocol was adopted as reported by Zhang et al.[26] Herein, in this modification a milder oxidizing agent, potassium dichromate was used. Briefly, 0.06 g of pristine MWCNT was dispersed in 12 mL of dichloromethane by sonication for about 10 min. An amount of 0.5 g phase transfer catalyst (cetrimide) is added to the mixture and sonicated for another 20 min, followed by addition of 2.5 mL of acetic acid and 2.5 g of potassium dichromate in small lots for about 2 h. The reaction mixture was stirred vigorously for 72 h at room temperature. The modified MWCNT was then obtained by filtering and by washing with concentrated acid, followed by distilled water and acetone. The modified MWCNT was dried in a vacuum oven at 40–45 °C for 24 h before using. The product used as functionalized and purified MWCNT.

2.3. Preparation of Diglycidyl Ether Bisphenol-S Epoxy Resin

Mesua ferrea L. seed oil based sulfone epoxy resin was prepared by the similar method as reported earlier.[12] Briefly, monoglyceride of the oil (obtained by glycerolysis technique), epichlorohydrin, bisphenol-A (BPA) and bisphenol-S (BPS) were reacted together by maintaining the mole ratio of 1:5:2:1 at (110 ± 5) °C for 14 h in slightly alkaline medium. The resinous product was isolated, washed and purified. The purified and dried product is coded as BPSE.

2.4. Fabrication of Nanocomposites

At first the functionalized MWCNT was vacuum dried at (40–45) °C for overnight. The nanocomposites were then prepared by incorporation of pre-calculated amount (1–3 wt% with respect to resin) of MWCNT in the BPSE matrix. The components were mixed together by hand stirring followed by sonication (pulse cycle 0.5 and amplitude 55–60%) for about 45 min. To avoid the rise of temperature during sonication, water bath was used to maintain the temperature at 25–30 °C. The dispersed MWCNT/resin system was degassed for 30 min under vacuum before further processing. The prepared nanocomposites are coded as ECN1, ECN2 and ECN3 for 1, 2 and 3 wt% of MWCNT loadings in the matrix.

2.5. Curing of the Resin and Nanocomposites

A homogenous mixture of the BPSE and nanocomposites with 50 phr (parts per hundred gram with respect to epoxy resin) of poly(amido amine) hardener was prepared separately in a glass beaker at room temperature by vigorous stirring for 20 min. A high vacuum was applied for about 15 min to remove any volatile generated during the mixing. The thin film of the mixture was casted on a glass plate and kept for 2 h under ambient conditions. The plates were then heated at 100 °C in a muffle furnace to determine the touch free time (minimum time, when no impression will appear on touching the film) and hard dry time (when no indentation on the film can be made by nail of the thumb) of the pristine resin and the nanocomposites. The mixtures were also uniformly spread on mild steel plates (150 mm × 50 mm × 1.60 mm), tin plates (150 mm × 50 mm × 0.40 mm) and glass plates (75 mm × 25 mm × 1.75 mm) for impact strength, gloss and scratch resistance tests.

2.6. Biodegradation by Broth Culture Technique

An inoculum was prepared by growing bacteria in 50-mL Erlenmeyer flasks containing 10 ml of nutrient broth (peptone 5 g/L, beef extract 1.5 g/L, NaCl 5 g/L, yeast extract 1.5 g/L) at 37 °C, pH-7.0, and at an agitation speed of 200 rpm. Then 1 mL of inoculums of bacteria containing an approximate 1×10^8/mL

microbes (as calculated from McFarland turbidity method) was inoculated into the conical flask containing 100 mL nutrient broth (without any carbon source) for each test with experimental nanocomposites films. Media containing no polymer film were also cultured as negative control. The flasks were then incubated under sterile condition at an agitation speed of 200 rpm at 37 °C for the degradation study. The samples were collected for spectrophotometric observation at 600 nm against blank culture media on weekly basis under sterile condition. Bacterial growth was calculated from the absorbance data using McFarland turbidity as the standard. Bacillus subtilis strain was selected as the model organism for the study.

2.7. RBC Haemolysis Protection Assay

The haemolytic activity test was done to see if the nanocomposites have any haemolytic activity on the erythrocytes based on the modified protocol as reported by Plumel.[27] Goat blood (100 mL) was collected in a container containing 10 mL of 3.8% tri sodium citrate solution. The mixture was then centrifuge for 15 min at 2,500 rpm under ice cold condition (4 °C). After centrifugation serum fraction was removed with disposable plastic transfer pipette and precipitate was re-dissolved in 0.9% NaCl solution, it was repeated for 4–6 times. After removing NaCl after the last wash step, the whole blood was mixed with 100 mM potassium phosphate buffer (PB) at pH of 7.4. RBC was then diluted to a ratio of 1:10 with phosphate buffer so as to yields a RBC suspension of $\sim 5 \times 10^8$ RBC/mL

RBC haemolysis protection assay was carried out according to Zhu et al. with little modification.[28] In brief, 10 mg of the nanocomposites was put into 2 mL of RBC suspension and incubated at 37 °C in water bath. About 200 μL of the suspension was taken out at an interval of 2 h and diluted eight times with PB and was continued for 6 h. The absorption was measured at a wavelength of 415 nm taking the supernatant liquids obtained after centrifuging at 3000 rpm for 10 min at 25 °C. The PB blank solution was taken as a reference.

2.8. Measurements

FTIR spectra of resin, unmodified MWCNT and functionalized MWCNT and nanocomposites were recorded in FTIR spectroscopy (Impact-410, Nicolet, USA) using KBr pellet. The surface morphology of the samples was studied by a JEOL scanning electron microscope (JSM-6390LV SEM) after platinum coating on the surface. Wide angle X-ray scattering (WAXS) studies were carried out using a powder diffractometer Rigaku X-ray diffractometer (Miniflex, UK) at room temperature (about 25 °C), operated at 30 kV and 15 mA. The scanning rate used was 2.0 min^{-1} over the range of $2\theta = 0$–$60°$ for the above study. The distribution of MWCNT in the polymer matrix was studied by using JEOL, JSM-1000CX transmission electron microscope (TEM).

The scratch hardness test (ASTM D5178/1991) of the cured films was done by using scratch hardness tester (Sheen instrument Ltd., UK). The front impact resistance test was carried out by applying falling ball method using an impact tester (S.C. Dey Co., Kolkata) with a maximum test height of 100 cm. In this test a weight of 850 g was allowed to fall on the film coated on a mild steel plate from minimum to maximum falling heights. The maximum height is taken as the impact resistance up to which the film is not tearing out.

The tensile strength and elongation at break (as per the ASTM D 412-51 T) were measured with the help of Universal Testing Machine of model Zwick Z010 (Germany) by using 10 kN load cell and at 40 mm/min jaw separation speed.

The adhesive strength of the cured thin films was measured by lap-shear test as per the standard ASTM D3165-95 using plywood, aluminium (Al), and polypropylene sheets as the substrates. The plywood substrates were first washed with acetone to remove dirt and subsequently polished with sand paper of grit number 60 (250 mm) according to ASTM 906. The clean Al sheets were treated with hydrochloric acid (5% w/v) and then washed with distilled water and dried.

Thermogravimetric (TG) analysis was carried out in Shimazdu TG 50 thermal analyzer using the nitrogen flow rate of 30 mL/min and at the heat rate of 10 °C/min.

3. RESULTS AND DISCUSSION

3.1. Functionalization of MWCNT

Carbon nanotubes has high tendency to agglomerate due to the van der Waals force, consequently it is very difficult to dispersed and align MWCNT in the polymer matrix. Thus to develop high performance MWCNT/epoxy nanocomposites the challenge is to disperse CNTs uniformly in the polymer matrix so as to achieve high interfacial interactions between the two phases. Nanotube functionalization the most effective way to achieve good dispersion and interphase control within the matrix polymer, consequently better stress transfer from the polymer to tubes effectively enhances the mechanical properties of the nanocomposites.[29] The oxidation of MWCNT by acidic oxidative methods, oxygen plasma or gas phase treatment has gained lots of attention in an attempt to purify and enhance the chemical reactivity of the graphitic network.[30] As already mentioned,[29, 30] acidic oxidative treatment to the MWCNT material may severely affect its structural properties. Especially, pristine MWCNT exhibit significant lack of conjugation and some precaution should be taken for the purification/surface modification of this materials.[30] This may lead to an appreciable etching of the carbon material even under moderate oxidation conditions. In order to transfer the optimum properties of MWCNT to their composites, the main challenge is the preparation of highly purified material with no appreciable structural damage. Thus MWCNT was functionalized under mild conditions using $K_2Cr_2O_7$ in the presence of phase transfer catalyst under ambient condition. This causes functionalization (–OH/–COOH) without deterioration of tubes aspect ratio.

3.2. FTIR Analysis

FTIR spectroscopy is an important tool to identify various functional groups present on the graphitic surface of MWCNT. The modification of the graphitic network of the MWCNT can be depicted from the FTIR spectra (Fig. 1). The pristine MWCNT exhibits band at 1639 cm^{-1} which is assigned to the C═O stretching of the quinone groups on the surface.[31] The presence of band at around 3433 cm^{-1} is due to the –OH stretching vibrations. After treatment a broad band for –OH stretching appeared at 3487 cm^{-1} and aliphatic –OH bending appeared at 1447 cm^{-1}. Further, two new bands were observed at around 1719 and 1095 cm^{-1} (Fig. 1), which are attributed to –C═O and –C–O stretching vibrations of the carboxylic acid group (–COOH) respectively. Furthermore, new bands were also observed at 2922, 1262/1165 cm^{-1}, mainly attributed to the –CH stretching and

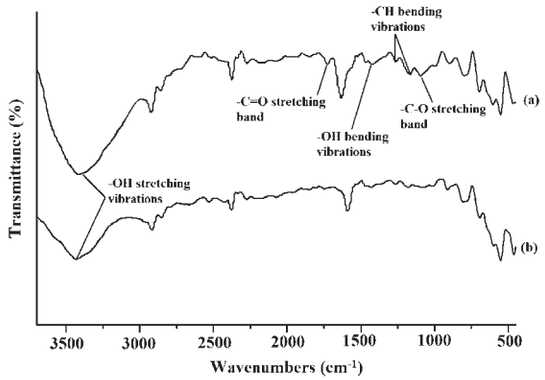

Fig. 1. FTIR spectra, (a) unmodified MWCNT and (b) modified MWCNT.

bending modes.[32] The FTIR study suggested the carboxyl and hydroxyl functionalization on the MWCNT surface.

These induced carboxyl/hydroxyl functionality on the MWCNT surface is expected to enhance the interaction with the BPSE matrix. The FTIR spectrum of epoxy resin is documented in our earlier published report.[14] Some of the characteristic bands (cm^{-1}) observed were: 3423 (–OH stretching vibrations), 3050 (aromatic C–H stretching vibration), 1729 (C═O stretching vibration of the triglyceride esters), 1593 (C═C stretching vibration), 1300 and 1149 (sulfone stretching vibrations), 1246 and 1106 (C–O–C stretching vibrations), and 916 and 832 (oxirane ring stretching vibrations). The FTIR spectra of the nanocomposites are shown in Figure 2. With the increase of the MWCNT loading the –OH absorption band of BPSE exhibits a red shift with simultaneous reduction in the band intensity. The –C═O stretching band however, appeared as a broad band in the region of 1619–1647 cm^{-1}, may be due to the overlapping of the –C═O stretching vibrational band of the quinone group of MWCNT with the –C═O stretching band of the triglyceride ester moiety of BPSE, with reduction in band intensity. The crosslinking of the epoxy resin with amine hardener in presence of MWCNT suggest extensive amount of interaction present in the system. The interaction of the –C═O group of the CNT surface with the epoxy group through H-bonding enhances the interaction of the $–NH_2$ group of the hardener. Moreover, the –OH group of BPSE is involve in H-bonding with the –C═O

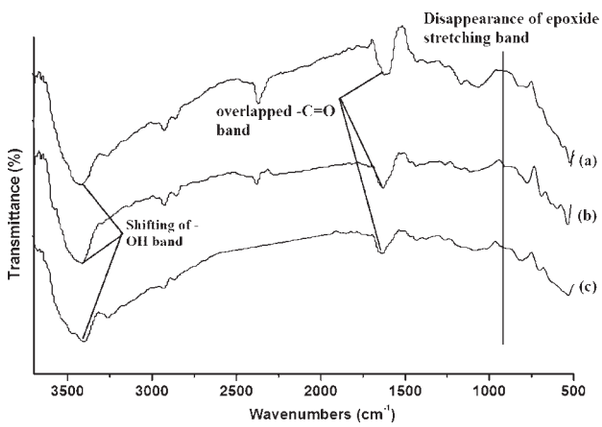

Fig. 2. FTIR spectra of MWCNT/BPSE nanocomposites: (a) ECN1, (b) ECN2 and (c) ECN3.

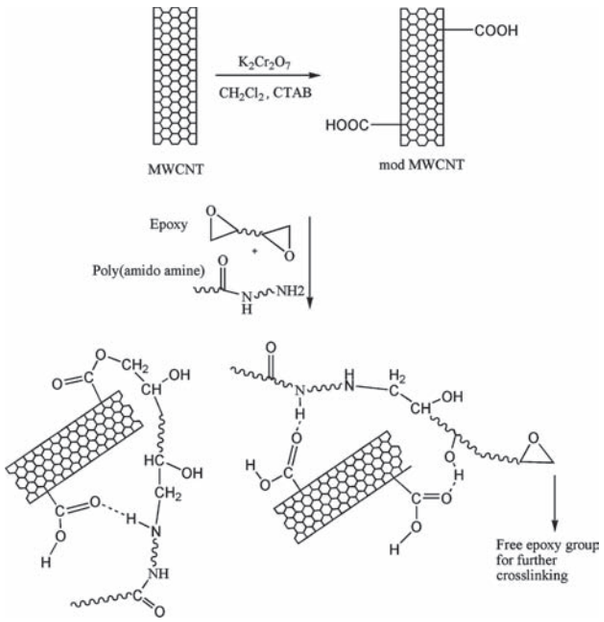

Scheme 1. Probable interaction of MWCNT with BPSE matrix.

group of the CNT (Scheme 1). Thus, the poly(amido amine) hardener also served as a compatibilizer between the epoxy and the MWCNT. The oxirane stretching vibration (916 cm^{-1}) in all the composites diminishes after curing. This indicates the completion of curing reaction of the epoxy resin via ring opening of the oxirane group. These interactions altogether facilitates the stable dispersion of the MWCNT in the epoxy matrix.

3.3. Dispersion of MWCNT

It is well known[30] that MWCNT have a strong tendency to agglomerate due to their nano size and their respective high surface energy. Dispersion of MWCNT in polar aprotic solvent is shown in Figure 3. Pristine MWCNT were quickly precipitated

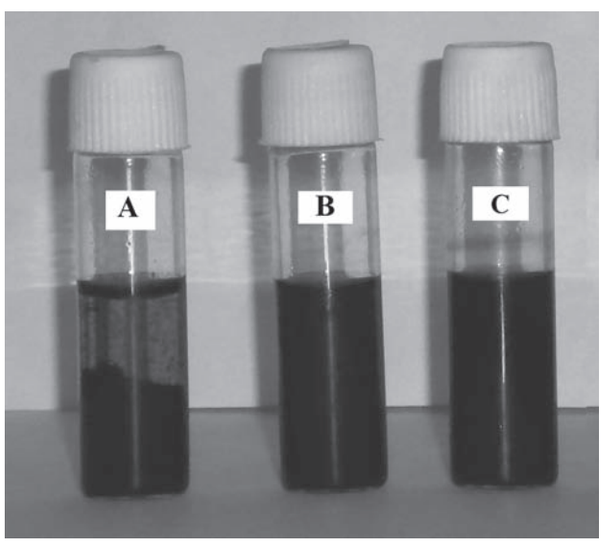

Fig. 3. Dispersion stability of (A) unmodified MWCNT, (B) modified MWCNT in DMF and (C) modified MWCNT in DMAc.

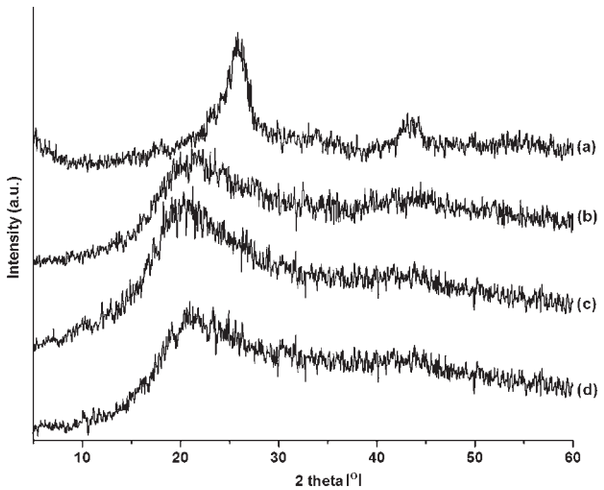

Fig. 4. XRD spectra (a) modified MWCNT, (b) ECN1, (b) ECN2 and (c) ECN3.

in DMF solution even after sonication for 30 min; however, the MWCNT showed good dispersion in DMF solution even after 72 h. The MWCNT were also dispersed in DMAc, the stability of each of the dispersion was found to be enhanced after modifications. This phenomenon of uniform nanotube dispersion in solvents is one of the properties of functionalized nanotubes. It has been reported that due to the nanoscale size, the high surface energy of nanotubes gives them a strong tendency to agglomerate. Even with the help of ultrasonic vibration, the untreated nanotubes may not remain in any solvent in quiescent suspension. However, appropriate functionalized nanotubes can dramatically raise the stability of suspensions.[26] The functionalization process induces a negatively charged surface, particularly through the ionization of acidic surface groups. The resulting electrostatic repulsion leads to the stable uniform colloidal dispersion.

3.4. XRD Analysis

The X-ray diffraction results for the nanocomposites are shown in Figure 4. The X-ray diffraction pattern of the functionalized MWCNT revealed the presence of two crystalline peaks at $2\theta = 25.8°$ and 42.8°, corresponding to the interlayer spacing of 0.34 nm. These are due to (002) and 0.21 nm due to (100) planes of the carbon atoms, respectively.[33] The spectra of the nanocomposites reveals no peak for the MWCNT, however a broad peak is found around 19.9° in the spectra of nanocomposites, which is due to the amorphous nature of the BPSE matrix. However, in this study, a small amount of carbon nanotubes (3 wt%) was used for preparing the epoxy nanocomposites and hence no X-ray diffraction peak for MWCNT in the nanocomposites, may also be one of the reason.

3.5. Morphological Characterizations

The morphology and spatial distribution of the MWCNT in the epoxy matrix were examined with the help of SEM and TEM analyses (Figs. 5 and 6). The platinum coated surface of the sample was observed in SEM. The random distribution of the nanotubes in the epoxy matrix can be distinctly viewed from Figure 5. The polymer embedded MWCNTs appeared as tiny bright thread like lines in the micrographs. The bright lines increase with the increase of MWCNT loading. Interestingly, no aggregate or agglomerates was observed nanocomposite with different MWCNT concentrations. This is the effect of chemical modification of the MWCNT that facilitates of wetting by the BPSE and phase adhesion between the phases.[34] This homogeneous dispersion of the MWCNT in the matrix will definitely

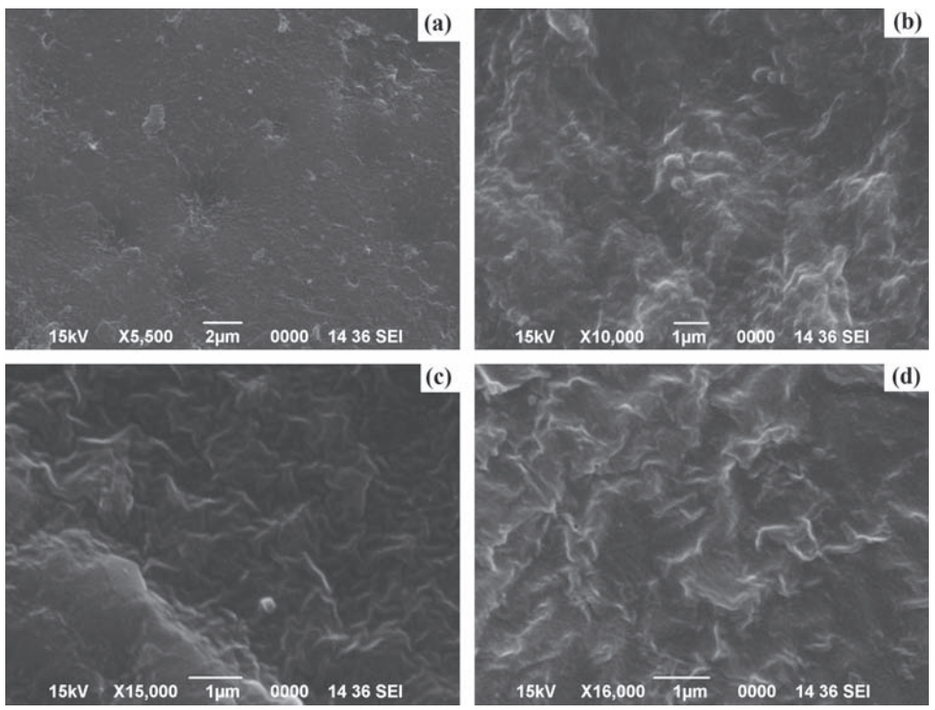

Fig. 5. SEM mircographs for (a) BPSE, (b) ECN1, (c) ECN2 and (d) ECN3.

enhance the properties. Thus, the MWCNT has been successfully dispersed in the vegetable oil based matrix. The homogeneous dispersion was maintained even after the cure of the resin.

The TEM micrograph gives further evidence of the fine dispersion of the MWCNT in the epoxy matrix. The representative TEM micrograph of ECN3 is shown in Figure 6, the presence of individual tubes proves the debundling of the MWCNT's. The visibly dark line represent the nanotubes, the uniform dispersion of the tubes reveals good interaction between the matrix and the tubes.

3.6. Curing Study

The influence of MWCNT loading on the curing process of BPSE is depicted in Table I.

The initial curing was found to accelerate with MWCNT loading as indicated by the touch free time (Table I). ECN3 exhibited the lowest cure time among the studied system. In the early stage, the reaction is initiated by any hydrogen-bond donor molecules which can be moisture, impurities. The reaction is then accelerated by these molecules and the hydroxyl groups formed during the reaction (as revealed by FTIR spectra). In the last stage, the viscosity of the mixture increase significantly and the reaction is diffusion-controlled.[35] Consequently, the hard dry time does not show any significant variation on MWCNT loading. The high cure rate obtained in the initial phase could be counter balanced by the rapid decrease of the cure in the diffusion-controlled stage. Lower or comparable cure degrees of the composites compared to the resin are was obtained.

3.7. Thermal Stability

The thermo-gravimetric profile of the BPSE and the nanocomposites is shown in Figure 7. MWCNT have been known to exhibit superior thermal stability.[34] The incorporation of MWCNT in the polymer matrix has a significant effect on the thermal stability of the nanocomposite as evident from Figure 7. The thermal stability increases with the increase of MWCNT loading. BPSE shows onset degradation temperature of 277 °C, whereas the onset degradation temperature shifts to 293 °C for ECN1, 302 °C for ECN2 and to 318 °C for ECN3. The strong interaction between MWCNT and epoxy matrix, diffusion of small molecules through the matrix is greatly reduced[36] at high temperature. Addition of 1 wt% of nanoclay results in about 16 °C enhancement in the onset temperature. MWCNT acts as a thermal insulator, which has strong interfacial interaction between the epoxy chains thus retarding the segmental mobility of the chains. The higher weight residue of the nanocomposites as compared to BPSE, further justify the above statement. As evident from Figure 7, for ECN3 the weight residue at 650 °C is about 16.97%, ECN2 shows 14.9% and ECN1 exhibits weight residue of 8.37%, whereas for BPSE it is only 6.65%. The char acts as a thermal insulator, thereby preventing the underlying matrix from volatization and consequently enhancing the degradation temperature.

Table I. Curing time of BPSE and MWCNT nanocomposites.

Sample code	Touch free time (min)	Hard dry time (min)
BPSE	45	65
ECN1	37	63
ECN2	30	64
ECN3	22	65

3.8. Mechanical Properties

The mechanical property depends on various factors such as state of distribution of the filler, aspect ratio, shape and size of the different domains and of course their orientations. MWCNT exhibits high strength properties. The interfacial interaction between MWCNT and the matrix is the measurement of the increment in the strength properties of the nanocomposites.[34]

The mechanical properties of the pristine polymer and the nanocomposites are shown in Table II. The inclusion of 3 wt% of MWCNT significantly increases the tensile strength from 6 to 15.4 MPa (Table II). The nanoscale dispersion of the CNTs into individual layer plays a multifold role in enhancing the tensile strength of the nanocomposites. The homogeneously dispersed tubes provide a greater degree of interfacial bonding between the polymer chains and the tube surface.[37] BPSE lacks sufficient tensile strength because of less chain entanglement. A good interface is eminent for a material to stand the stress. A strong bond reflects efficient stress transfer in the interface between the two

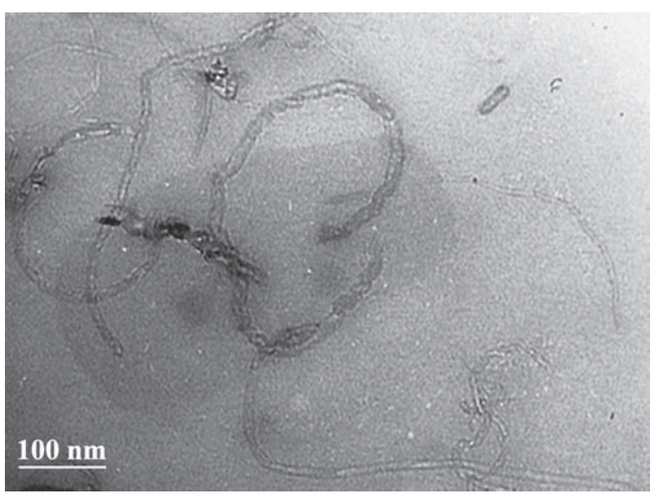

Fig. 6. TEM image of ECN3.

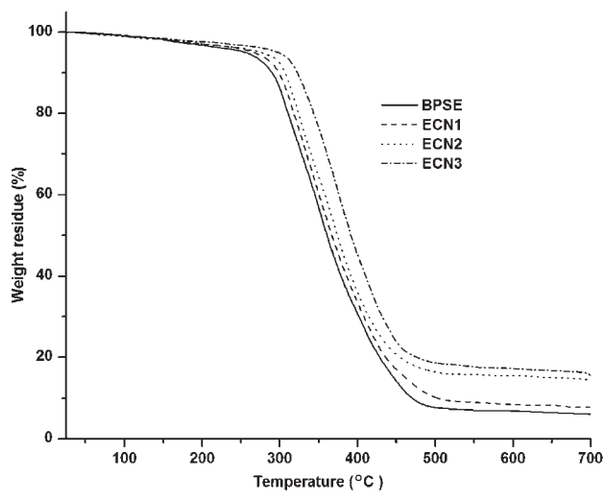

Fig. 7. Thermo-stability of BPSE and MWCNT nanocomposites.

Table II. Performance characteristics of BPSE and its MWCNT nanocomposites.

Sample code	BPSE	ECN1	ECN2	ENC3
Tensile strength (MPa)	6	8.4	12.3	15.4
Elongation at break (%)	95	103.4	110.4	126.3
*Impact resistance (cm)	100	100	100	100
Scratch hardness (kg)	3.4	4.7	6.2	7

Note: *100 cm is the maximum limit of the instrument.

phases, which increases with MWCNT loading. Thus, the room temperature modification of the MWCNT is found to be efficient in reinforcing the matrix. The elongation at break value for the nanocomposites has been found to increase as compared to the pristine polymer. The increase in the elongation at break depends on the state of dispersion of the nanotubes in the matrix polymer. The surface functionalization induces chemical bonding (covalent bonding, van der Waals forces, *p*-stacking) of the carbon structure of the CNTs with the molecular structure of the thermosetting matrix, this result in efficient load transfer. Elongation at break depends more seriously on the internal bond strength rather than crosslinking density and the phenomenon is guided by chain breakage rather than chain slippage.

The scratch hardness also augments with the MWCNT loadings. The increase in scratch hardness is due to the dissipation of the stress generated at the interface between the moving tip and the film surface throughout the nanocomposite. The stress is than absorbed by the nanotubes and consequently scratch hardness increase in this case.

3.9. Adhesive Study

To determine the influence of the surface of substrate on the adhesive strength of BPSE and the nanocomposites different substrates such as plywood, aluminium and plastic were taken. The average lap shear strength values of the specimens with different MWCNT loadings are shown in Figure 8. The shear stress of each MWCNT weight fractions was repeated three times and the results were repeatable within deviations of ±3.5%. The adhesive strength shows the highest value for the wood substrate and

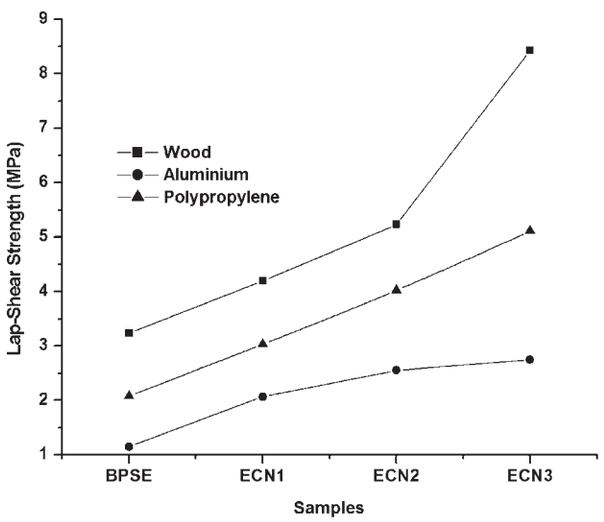

Fig. 8. Lap shear adhesive strength of BPSE and MWCNT nanocomposites on different substrate (wood/aluminum/polypropylene).

it increases with the increase in the MWCNT content (8.4 MPa in case of ECN3). Uniformly dispersed MWCNT have certain effects on the physical and chemical properties of the adhesion for epoxy adhesive. They provided stronger anchoring and hence increased adhesion strength by virtue of their positioning in the surface asperities of the wood surfaces.[38] Adhesive or cohesive forces may be attributed to either short or long range interactions. The increment of adhesive strength is due to the strong interactions of polar hydroxyl, epoxy, ether and other polar groups of the BPSE/MWCNT nanocomposite with the hydroxyl groups of the substrate. The interactions are through hydrogen bonding, polar–polar and polar-induced-polar interactions, or/and chemical bond formation. BPSE also shows good adhesion on to the metal substrate. The lap shear strength exhibits a continuous increase with MWCNT loading. ECN3 exhibits 145 percent increase in lap shear strength for Al substrate. Virtually all common metal surfaces exist as hydrated oxides. Thus the adhesive used for these materials must firmly interact with the metal oxide layer. The plausible explanation for good adhesion on to the steel substrate may be due to better interlocking and formations of secondary bonds with the rough surface of metal, aided by the induced functionality (hydroxyl/carboxyl, etc.) on the MWCNT after modification.[39] Poor adhesive strength was observed in case of polypropylene substrate, compare to wood and aluminium substrates. This result suggests that the surface treatment of the polypropylene with HNO_3 may generate active sites for interaction with the matrix, but that are still not enough compared to wood or aluminium substrate.

3.10. Biodegradation

A striking aspect of epoxy resin is their non-biodegradability under ambient conditions. Broth culture technique was used to study biodegradability of *Mesua ferrea* L. seed oil modified epoxy resin the MWCNT based nanocomposites.

The growth profiling of consortia in the modified broth media lacking carbon source compels the bacteria to use epoxy and nanocomposites as the primary carbon source in each case.[40]

The biodegradation of BPSE and its nanocomposites were quantitatively tested and confirm by direct exposure to strain of *bacillus sp.* bacteria by broth culture technique. The growth of *bacillus sp.* bacterial strain on epoxy system and various nanocomposites films can be realized from Figures 9 and 10, respectively. After keeping the samples in broth culture media for six weeks, the bacterial OD was determined. The difference in the rate of growth initially for two weeks both for the nanocomposites as well pristine system is not significant as can be seen from the curves after two weeks of bacterial exposure (Fig. 9). However, the bacterial growth rate increases significantly after two weeks, as can be realized from the bacterial count. The inoculated films were found to deteriorate significantly after two weeks (Fig. 10). Again, the rate of biodegradation was found to be higher than the corresponding pristine polymer in both the cases (Fig. 9). The presence of the vegetable oil moiety in the epoxy structure plays an important role in assisting the microbial degradation of the systems. The surface topography as visualized by SEM in the case of treated samples exhibits deteriorations of structure integrity. The presence of MWCNT was found to accelerate the rate of degradations.[41] The functionalized MWCNT accelerates the biodegradation by absorbing water, which helps the hydrolysis of the BPSE matrix in presence of the microbes, thus initializing the degradation of the matrix.

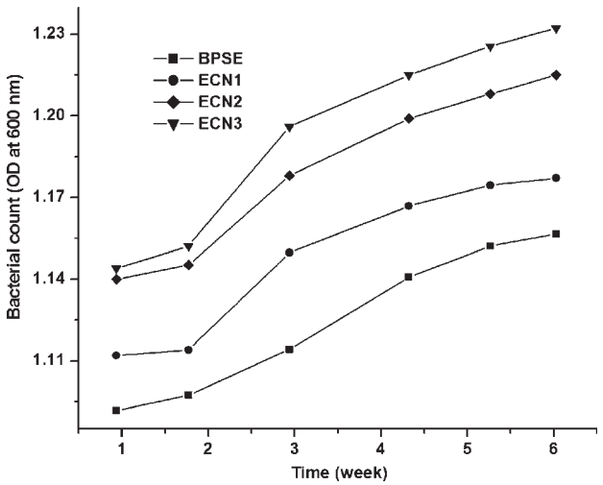

Fig. 9. Statistics of growth of *bacillus subtilis* in BPSE and nanocomposites post 6 weeks of inoculations.

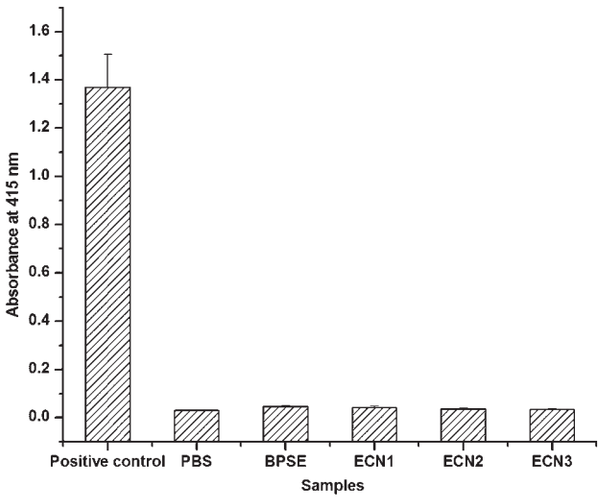

Fig. 11. RBC protection assay of BPSE and nanocomposites.

3.11. RBC Haemolysis Protection Assay

The emergence of nanotechnology also raises the question of safety from any possible toxic effect of nano structures.[34] Thus it is imperative to investigate the adverse effect of MWCNT based biomaterials before they may be forwarded for widespread acceptance and uses. Here, the cyto-compatibility for the BPSE and composites was investigated by RBC haemolysis protection assay and the results are shown in Figure 11. In the study water was taken as the positive control and PBS as the negative control. Examining the plots reveals the haemolysis prevention of the nanocomposites to be similar to that of the negative control. The test was carried out for 6 h and it was observed that after 3 h the inhibition capability starts to decline. The increasing saturation of MWCNT may be the reason for the decline.[27, 34] However up to six hours the nanocomposites retains sufficient inhibition capability. The nanocomposites showed dose dependent inhibition behaviour, and is a direct effect of the MWCNT. The films are non-cytotoxic as implied by the assessment. The composites prominently prevented the damage to the cell by the free radicals. This is due to the high free radical scavenging property of BPSE/MWCNT composites that react with free radicals, by two mechanisms viz., electron transfer process and adduct

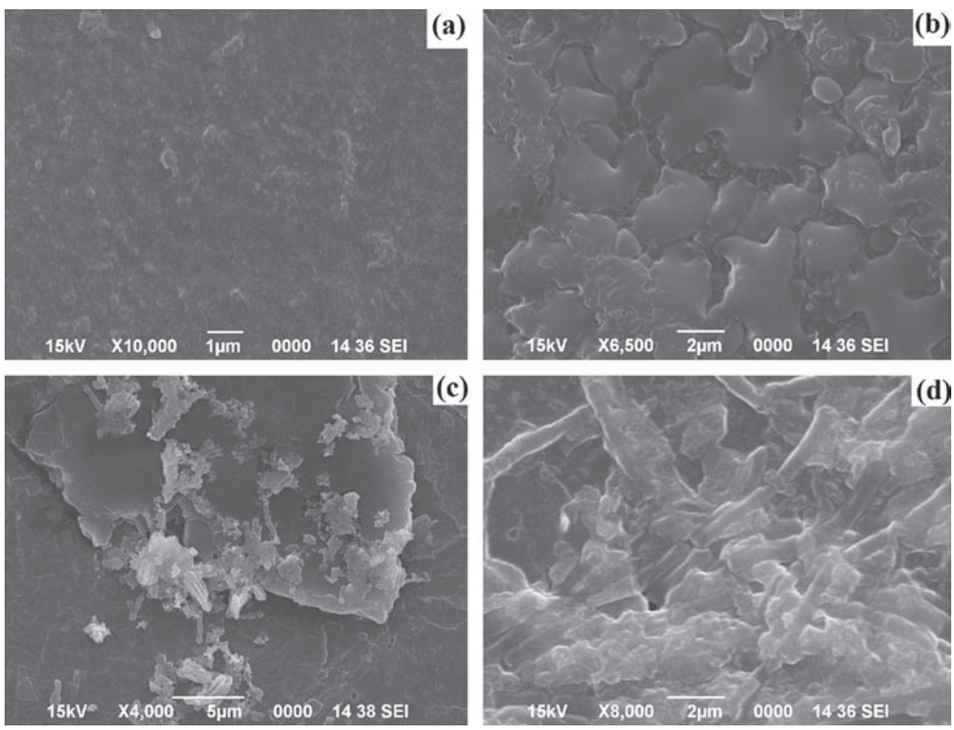

Fig. 10. SEM micrographs of (a) untreated BPSE and MWCNT/BPSE nanocomposites post 6 weeks of inoculations (b) ECN1, (c) ECN2 and (d) ECN3.

formation.[34] The virgin polymer shows less RBC haemolysis prevention capacity. This indicates that the MWCNT plays a crucial role in the RBC haemolysis prevention. Thus the study reveals that the nanocomposites are not only non toxic but are also capable of preventing the cell from the attack of harmful radicals.

4. CONCLUSION

From this study this can be concluded that the mild oxidative technique using phase transfer catalyst introduces sufficient functionality which aids in the good dispersion of the MWCNT in the *Mesua ferrea* L. seed oil modified epoxy resin. The homogeneous dispersion of the MWCNT was reveal by XRD, SEM, TEM and FTIR techniques. The nanocomposites showed enhancement in the mechanical properties and thermal properties with increasing MWCNT loading. The adhesive strength of MWCNT/BPSE nanocomposites tested on different substrate (wood/aluminium/polypropylene) tested by lap shear test methods shows sufficient strength of the bonded joint. The composite material has also displayed biocompatibility in terms of non-toxicity at the cellular level and biodegradability.

In view of these features, the MWCNT/BPSE nanocomposites may be viewed as a potential candidate for further exploration for determining their sustainability in biomedical applications such as in dentistry, tissue adhesive etc.

Acknowledgment: The authors express their gratitude to UGC for the financial assistance given for carrying out the work via. Sanction letter No. F. 16-1532(SC)/2009 [SA-III].

References and Notes

1. J. C. Suarez, I. D. Ulzurrun, M. V. Biezma, J. M. R. Romand, M. A. Martınez, J. C. Real, and F. Lopez, *J. Mater. Process. Technol.* 144, 219 **(2003)**.
2. S. Yu, M. N. Tong, and G. Critchlow, *Mater. Design* 31, S126 **(2010)**.
3. M. Shi, J. Zheng, Z. Huang, and Y. Qin, *Adv. Sci. Lett.* 4, 740 **(2011)**.
4. D. Katz, E. Brandeis, and J. Klein, US Patent no. 5266608 **(1999)**.
5. A. Sekulic and A. Curnier, *Int. J. Adhes. Adhes.* 30, 89 **(2010)**.
6. M. F. Harmand, L. Bordenave, R. Bareille, A. Naji, R. Jeandot, F. Rouais, and D. Ducassou, *J. Biomater. Sci. Polym. Edn.* 2, 67 **(1991)**.
7. A. Mubashar, I. A. Ashcroft, G. W. Critchlow, and A. D. Crocombe, *Int. J. Adhes. Adhes.* 29 751 **(2009)**.
8. D. E. Packham, *Int. J. Adhes. Adhes.* 29, 248 **(2009)**.
9. H. O. Metzger and M. Eissen, *Comptes. Rendus. Chimie.* 7, 569 **(2004)**.
10. C. A. Finch, Handbook of Adhesion, Wiley, Chichester **(2009)**.
11. E. Gruber and Wochent, *Fuer Papier Fabri. J.* 128, 594 **(2000)**.
12. A. J. Kinloch, Adhesion and Adhesives: Science and Technology, Chapman and Hall, London **(1987)**.
13. R. B. Janota, High-Performance Adhesive Bonding, Society of Manufacturing Engineers, Michigan **(1983)**.
14. G. Das and N. Karak, *Prog. Org. Coat.* 69, 495 **(2010)**.
15. H. Miyagawa, R. J. Jurek, A. K. Mohanty, M. Misra, and L. T. Drzal, *Composites: Part A* 37, 54 **(2006)**.
16. Y. Ando, *J. Nanosci. Nanotechnol.* 10, 3726 **(2010)**.
17. J. H. Lee and K. Y. Rhee, *J. Nanosci. Nanotechnol.* 9, 6948 **(2009)**.
18. Y. Ando and M. Kumar, *J. Nanosci. Nanotechnol.* 10, 3723 **(2010)**.
19. Y. Zhao, T. Tong, L. Delzeit, K. Ali, M. Meyyappan, and A. Majumdar, *J. Vac. Sci. Technol. B.* 24, 331 **(2006)**.
20. Y. Zhao, B. Mannhalter, H. Hong, and J. S. Welsh, *J. Nanosci. Nanotechnol.* 10, 5776 **(2010)**.
21. H. Miyagawa, A. K. Mohanty, L. T. Drzal, and M. Misra, *Nanotechnology* 1, 118 **(2005)**.
22. S. Wang, Z. Liang, T. Liu, B. Wang, and C. Zhang, *Nanotechnology* 17, 1551 **(2006)**.
23. H. A. Perez, F. Avile, F. P. J. Herrera, P. P. Bartolo, P. A. May, and G. A. Valadez, *Compos. Sci. Technol.* 68, 1422 **(2008)**.
24. S. Dutta, N. Karak, J. P. Saikia, and B. K. Konwar, *Biores. Technol.* 100, 6391 **(2009)**.
25. S. S. Mahapatra and N. Karak, *Prog. Org. Coat.* 51, 103 **(2004)**.
26. N. Zhang, J. Xie, and V. K. Varadan, *Smart. Mater. Struct.* 11, 962 **(2002)**.
27. Q. Y. Zhu, R. R. Holt, S. A. Lazarus, T. J. Orozco, and C. L. Keen, *Exp. Biol. Med.* 227, 321 **(2002)**.
28. M. Plumel, *Bull. Soc. Chim. Biol.* 30, 129 **(1949)**.
29. N. G. Sahoo, S. Rana, J. W. Cho, L. Li, and S. H. Chan, *Prog. Polym. Sci.* 35, 837 **(2010)**.
30. V. Datsyuk, M, Kalyva, K. Papagelis, J. Parthenios, D. Tasis, A. Siokou, I. Kallitsis, and C. Galiotis, *Carbon* 46, 833 **(2008)**.
31. P. C. Ma, S. Y. Mo, B. Z. Tang, and J. K. Kim, *Carbon* 48, 1824 **(2010)**.
32. X. Chen, J. Wang, M. Lin, W. Zhong, T. Feng, X. Chen, J. Chen, and F. Xue, *Mater. Sci. Eng.: A* 492, 236 **(2008)**.
33. S. Rana, N. Karak, J. W. Cho, and Y. H. Kim, *Nanotechnology* 19, 495707 **(2008)**.
34. H. Deka, N. Karak, R. D. Kalita, and A. K. Buragohain, *Carbon* 48, 2013 **(2010)**.
35. A. Allaoui and N. E. Bounia, *eXP. Polym. Lett.* 3, 588 **(2009)**.
36. Y. Hu, J. Shen, N. Li, H. Ma, M. Shi, B. Yan, W. Huang, W. Wang, and M. Ye *Compos. Sci. Technol.* 70, 2176 **(2010)**.
37. J. A. Kim, D. G. Seong, T. J. Kang, and J. R. Youn, *Carbon* 44, 1898 **(2006)**.
38. H. Deka and N. Karak, *Polym. Adv. Technol.* 26, 973 **(2009)**.
39. E. M. Petrie, Handbook of Adhesive and Sealants, Mcgraw-Hill, New York **(2000)**.
40. R. S. Sinha and M. Okamoto, *Prog. Polym. Sci.* 28, 1539 **(2003)**.
41. T. Rafeeqi and G. Kaul, *Adv. Sci. Lett.* 4, 536 **(2011)**.

Received: xx Xxxx xxxx. Accepted: xx Xxxx xxxx.